



PERFORATED MUFFLER MANIFOLD CATALYST

K. R. NORMAN

Ford Motor Company, Dearborn, MI 48121, U.S.A.

A. SELAMET

*Department of Mechanical Engineering, The Ohio State University, Columbus, OH 43210,
U.S.A.*

AND

J. M. NOVAK

Ford Motor Company, Dearborn, MI 48121, U.S.A.

(Received 24 October 1997, and in final form 2 July 1998)

An alternative exhaust manifold system, the Perforated Manifold, Muffler, and Catalyst (PMMC), is proposed to improve sound suppression while reducing engine pumping losses and exhaust emissions. One-dimensional predictions from acoustic theory are used to configure the initial design. Preliminary evaluation of the concept is based on bench tests, including an extended impedance tube set-up for acoustic attenuation and a flow bench for flow loss characteristics. Experiments with the fabricated hardware are then conducted in an engine dynamometer facility, and the results were compared to the existing production system as a benchmark. Engine experiments show that the PMMC concept provides enhanced upstream sound suppression, reducing the need for restrictive downstream silencers. This results in reduced engine pumping work and thus improved engine brake horsepower. Additionally, conservation of exhaust gas thermal energy and the reduced thermal inertia of the exhaust system provides earlier catalyst light-off, and therefore reduced pollutant emissions.

© 1998 Academic Press

1. INTRODUCTION

Automobile manufacturers are striving to improve the performance of internal combustion engine powered vehicles. One of the systems that has a significant effect on the engine performance and compliance of the vehicle, and therefore presenting a potential for further development, is the exhaust. Upon opening of the exhaust valve, the blow-down process occurs, and the burned gases leave the cylinder at relatively high pressure and temperature. Large pressure fluctuations propagate as the gases undergo rapid accelerations and decelerations as a result of interaction with the manifold geometry and the other cylinder exhaust ports and runners. Sound levels measured at the exhaust port of an internal combustion engine may be as high as 190 dB. Left unattenuated, these large pressure variations would propagate downstream and radiate to the environment at very uncomfortable levels. The objective of the exhaust system is then to provide noise

silencing along with pollutant emissions compliance. It is equally important that these environmental objectives be achieved without significant impingement on the vehicle performance. A desirable exhaust system would have low weight and low back pressure for good engine performance and fuel economy, while providing low emission and sound levels.

The exhaust noise is usually reduced by using passive techniques that suppress the pressure waves. Typical passive reactive elements such as mufflers and resonators rely on reflections from geometrical changes, which are quite effective in reducing noise to acceptable levels for the frequency ranges of interest in automotive applications. However, these structures require valuable space, add weight and cost to the vehicle, and increase the back pressure to the engine leading to reduced net engine output. The increased back pressure is a result of the large flow losses inherent in the repeated flow separations, and can be alleviated to some degree through the use of perforated tubing. The objective of the present study is to investigate and design an alternative exhaust system to reduce sound levels through less restrictive structures. This is accomplished by incorporating exhaust components, such as a perforated manifold, muffler, and catalyst, into a single unit, the perforated manifold, muffler, and catalyst (PMMC) concept [1]. The PMMC replaces the usual manifold with a perforated tube expansion after the exhaust ports, just prior to collection in the catalyst, as shown in Figure 1. The perforated runners are housed by a volume of about 2.5 l. Acoustic improvements are expected because of the early expansion chamber effects in the system [2, 3]. The PMMC configuration also enhances engine performance and pollutant removal by carefully managing the flow through the manifold region. The grazing flow in perforates reduces flow losses due to expansion and also guides the flow to the catalyst. Perforations are applied to the low pressure areas of the exhaust runners to assist in keeping the flow attached on the inner walls of the pipe bends. Engine performance is improved due to a decrease in pumping work through reduced back pressure and flow losses [4]. Guiding the flow also reduces the flow contact with external walls, hence conserving the available thermal energy in the exhaust stream during start-up, enhancing the performance of the catalyst.

This proposed PMMC system is evaluated against the existing vehicle production system of the 1992 Ford Escort Engine. The schematic of the complete exhaust configurations for both production and PMMC are shown in Figure 2 along with locations of interest for later comparison. The original production system employs a resonator and a high restriction three-pass expansion/perforate muffler, whereas the PMMC system utilizes only a low-restriction muffler.

Following the Introduction, sections 2 and 3 detail the analytical design methodology for acoustical and engine performance enhancements, respectively. Next, preliminary evaluations of the concept are made using acoustic bench experiments and flow bench experiments in sections 4 and 5, respectively. Section 6 describes engine dynamometer experiments used to measure exhaust noise suppression and engine performance under full-load firing operating conditions. Finally, section 7 summarizes the results and makes recommendations for further development of the concept.

2. DESIGN FOR ACOUSTICAL PERFORMANCE

One-dimensional linear acoustic theory is used to evaluate the potential designs. Basic silencer configurations, such as expansion chambers, Helmholtz resonators, and quarter wave resonators form the building blocks of complicated silencers in the exhaust system. A number of studies have been conducted which predict the performance of these silencers using the linear acoustic theory and compare the results with experiments [3, 5–8]. Due to its broad band attenuation, the expansion chamber is often a desirable silencer. Expansion chambers expose the wave to abrupt cross-sectional area changes, causing wave reflections, resulting in weaker pressure waves transmitted through the silencer relative to the original incident wave. Transmission loss, which is the logarithmic ratio of incident power to transmitted power, is given for expansion chambers by [5]

$$TL = 10 \log_{10} \left[1 + \frac{1}{4} \left(m - \frac{1}{m} \right)^2 \sin^2 kl_e \right], \quad (1)$$

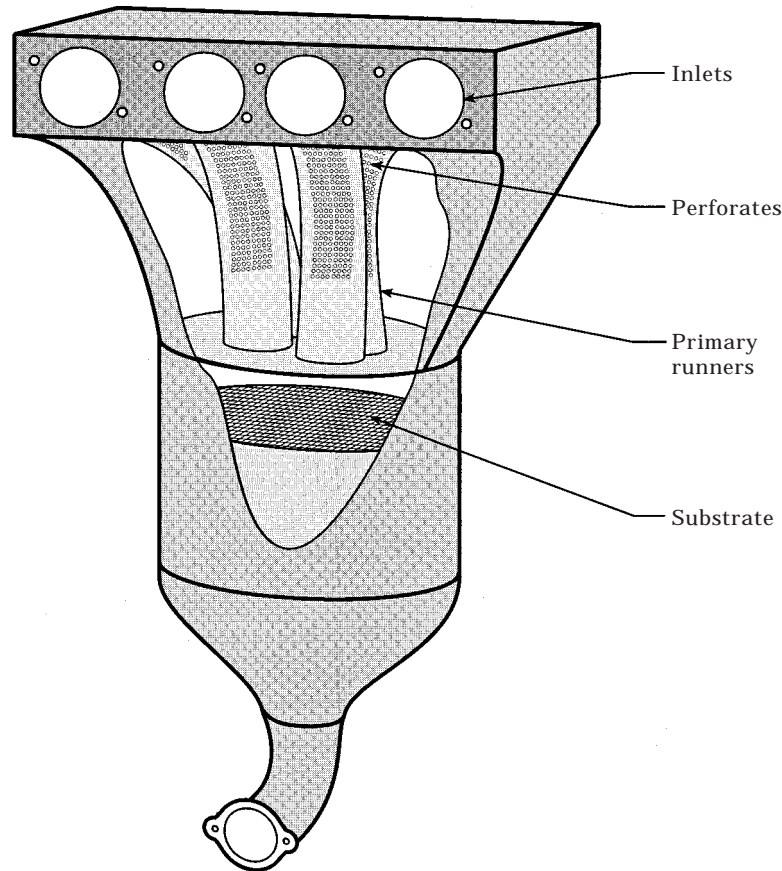


Figure 1. Schematic of the perforated manifold muffler catalyst unit.

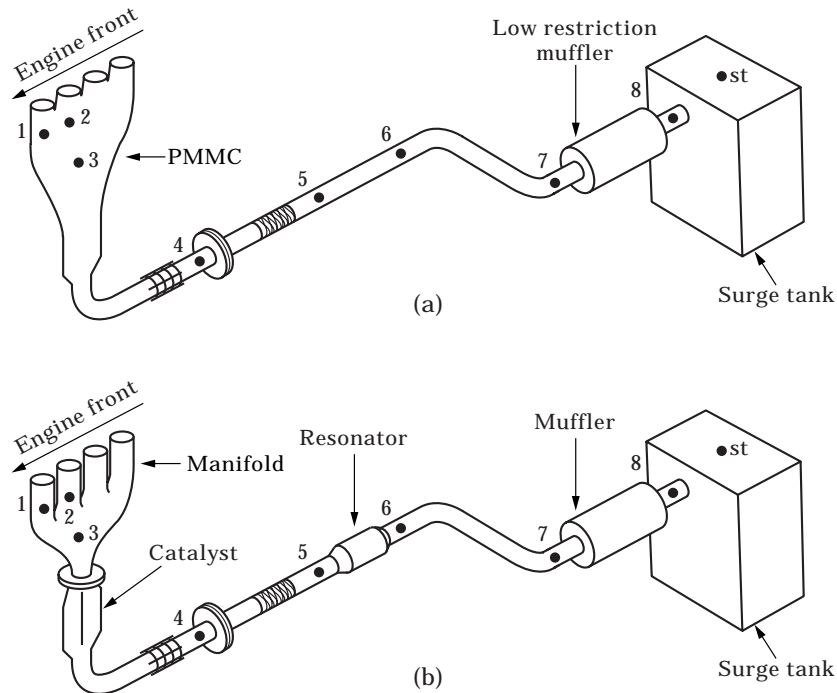


Figure 2. Schematic of (a) the PMMC and (b) production exhaust systems.

where $m = A_{\text{expansion}}/A_{\text{pipe}}$ is the expansion ratio, $k = 2\pi f/c$ is the wave number, and l_e is the length of the expansion chamber. Here, f is the frequency, c is the speed of sound, and $A_{\text{expansion}}$ is the cross-sectional area to which the wave from the pipe with cross-sectional area A_{pipe} is expanded. Equation (1) readily shows that: (1) transmission loss is increased with increasing expansion ratio: (2) the maximum transmission loss occurs at frequencies where odd multiples of the $1/4$ wavelength of sound are equal to the length of the expansion chamber ($f = nc/4l_e$, $n = 1, 3, 5, \dots$). This results from the wave being 180° out of phase after the reflection and therefore cancelling itself: (3) the maximum transmission loss occurs at frequencies with even multiples of the $1/4$ wavelength of sound equal to the length of the expansion chamber ($f = nc/4l_e$, $n = 0, 2, 4, \dots$). As a result, expansion chambers usually exhibit a familiar transmission loss behavior with repeating domes. For the expansion chamber of the PMMC, an approximate expansion ratio of 21.5 (based on the average of cross-sectional areas of the chamber at the inlet and the exit) and a length of 0.47 m were used for the estimates of transmission loss. These values, combined with the speed of sound ($c = 340$ m/s under ambient conditions), yield a maximum of about 21 dB at 181 Hz for the first dome.

The acoustic performance of the expansion chamber comes, however, at the expense of increased flow losses to the system when mean flow is introduced. To some degree, this effect can be alleviated using perforated tube silencers with an outer concentric tube surrounding them. The work of Sullivan and Crocker [9] suggests a porosity in the range of 5 to 10% to achieve the expansion chamber

behavior. Thus, if the perforate area is sufficient, the pressure pulsations experience effectively an expansion chamber, while little flow loss is introduced because the mean flow grazes over the perforates. To retain the characteristic dome attenuation behavior, the silencer must be length controlled versus volume controlled [7, 10]. This depends on whether the concentric tube perforate arrangement acts as an expansion chamber or resonator, which is determined by comparing the first axial modal frequency of the cavity to that of the equivalent Helmholtz resonance frequency given by

$$f_r = \frac{c}{\pi} \sqrt{\frac{\sigma d_1}{t_{eff}(d_2^2 - d_1^2)}}, \quad (2)$$

as described in reference [9]. Here σ is the porosity of the tube, $t_{eff} = t_{wall} + \Delta t_{wall}$ is the effective thickness with t_{wall} being the actual wall thickness and Δt_{wall} a correction factor for the end effects, and d_1 and d_2 are the diameters of the inner and outer ducts, respectively. While there are numerous expressions for Δt_{wall} (see for example, Alster [11]), a simple relationship [9], $\Delta t_{wall} = 0.75d_{hole}$ (d_{hole} being the hole diameter), is used here for an approximate estimate of resonance frequency.

For short chambers in particular, the broad band expansion chamber attenuation will give way to multidimensional behavior at frequencies below the first cutoff mode. Because, as the expansion chamber length becomes shorter, multidimensional effects do not have sufficient distance to decay, and non-planar modes propagate. The frequency at which the transition to multidimensional behavior occurs is known to decrease with the l_e/D_e ratio. The number of complete expansion domes prior to the onset of multidimensional behavior, is given by [10]

$$n_D \leq 2.440 \frac{l_e}{D_e}, \quad (3)$$

where n_D is the number of complete attenuation domes before the onset of the multidimensional behavior.

In the PMMC prototype, the flow is guided to the catalyst using perforated tubes. Underhood size constraints on the PMMC dimensions place it narrowly in the range of length controlled or expansion chamber behavior. A desirable porosity was estimated to be about 7%, which required 200 holes of 1/8" diameter along each of the 20 cm long runners. The simple one-dimensional expansion chamber theory predicts the first dome over a frequency range of 0 to 362 Hz. The first Helmholtz resonance frequency is estimated from equation (2) as 382 Hz (again using $c = 340$ m/s), which is slightly larger than 362 Hz where the first dome ends. This comparison coupled with the observation that equation (2) underestimates the peak frequency [9] places the PMMC prototype within the region of length-controlled behavior. Note that the foregoing estimates for both the expansion chamber and the Helmholtz resonator involve several simplifications in approximating a complex geometry, therefore only the trend is emphasized. Acoustic bench experiments later in section 4 will quantify the trends observed here.

The PMMC is predicted to have good noise attenuation at frequencies below 1 kHz due to the expansion volume. Reductions in sound levels in the low frequency range are significant to the performance of an exhaust system for internal combustion engines. Consider, for example the 1.9L I4 engine (firing four times per two revolutions) running at 6000 rpm. The associated fundamental frequency of the blowdown pulses is then $f = (4/2)(6000/60) = 200$ Hz. This primary firing frequency as well as its several harmonics will be less than 1 kHz. Additional periodic sound disturbances associated with cylinder firing order could result from cycle to cycle interactions which would be at frequencies in $1/n$ (n are integer values) multiples of the firing frequency, and hence lower than the original. Therefore, most exhaust noise of interest occurs at frequencies less than 1 kHz. The need for downstream muffling with the PMMC system is reduced by the early noise attenuation in the exhaust flow path.

3 DESIGN FOR POWER/EMISSIONS PERFORMANCE

The ability of the PMMC system to use a low restriction muffler reduces the back pressure at the engine headface. One effect of back pressure on engine performance can be illustrated in terms of the in-cylinder pressure versus volume (P - V) diagram in Figure 3. The upper loop in Figure 3(a) represents work or indicated power as a result of the combustion process following the compression of the air/fuel mixture. The lower loop area is the negative work or pumping work required to intake the fresh air charge and discharge the exhaust gases. The upper curve forming the pumping loop [enlarged in Figure 3(b)] is a result of engine back pressure. When this pressure is reduced, the area enclosed by the loop, or, the pumping work required of the engine will decrease. Hence, the net power out of the engine will be increased. The PMMC concept thus attempts to reduce the flow losses in the exhaust system to lower engine back pressure.

The pumping work per power cycle is defined by

$$W_p = -(P_e - P_i)V_{disp}, \quad (4)$$

where P_e is an average exhaust back pressure, P_i is an average intake pressure, and V_{disp} is engine displacement. Assuming the same intake manifold pressures for all systems, only the difference in the exhaust back pressures will affect the pumping work. The exhaust pressure P_e may be expressed as the sum of the atmospheric pressure plus the back pressure due to flow losses in the exhaust pipe, $P_e = P_{atm} + \Delta P_{losses}$. Therefore, reducing pressure losses in the exhaust system, decreases the engine back pressure and in turn parasitic pumping work required of the engine.

Considering current pollutant levels from internal combustion engines and existing catalyst technology, additional improvements in emissions levels can be achieved by further reducing the catalyst light-off time. Gains in emissions performance of the PMMC system are expected primarily because of the predicted shorter light-off time due to reduced heat losses as compared with the production system. For catalytic converters to function, the temperature inside the brick must reach approximately 250°C before conversion reactions are initiated. The time

from the start of a cold engine until the converter reaches this operational temperature is frequently referred to as the light-off time. For quick light-off, the converter must recover as much of the energy from the exhaust stream as possible. By moving the catalyst upstream, less heat will be transferred away from the exhaust stream before the gases reach the reaction zone, which will reduce the light-off time. The reduced mass of the stainless steel PMMC design will result in

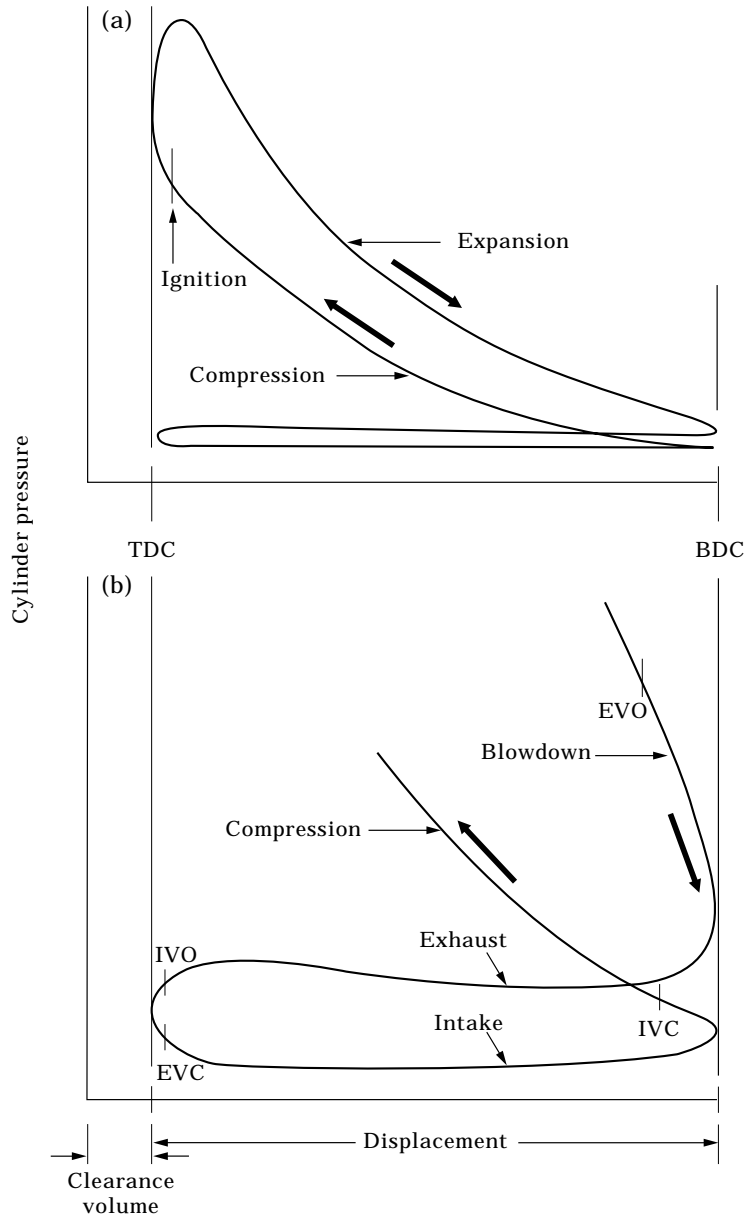


Figure 3. Example of an in-cylinder pressure versus volume ($P-V$) diagram: (a) total cycle, (b) expanded pumping loop.

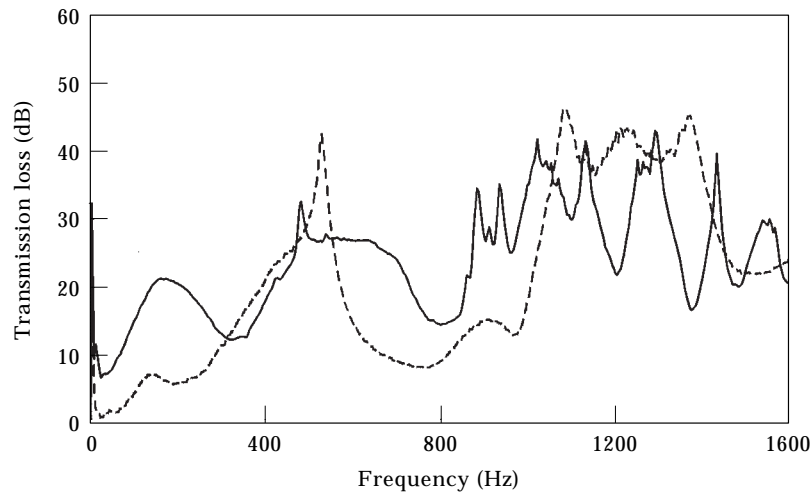


Figure 4. Transmission loss versus frequency for runner 1 of the manifold/catalyst systems: —, PMMC; ---, production.

a smaller thermal inertia upstream of the catalyst and will help improve the light-off time as compared to that of a standard cast iron manifold [12, 13].

4. ACOUSTIC BENCH EXPERIMENTS

It was desirable to measure silencing performance of the manifold chamber prior to final fabrication of the PMMC for engine testing. Noise attenuation experiments are conducted with a zero mean flow acoustic bench. Transmission loss across each system is measured on an extended impedance tube set-up under zero flow and ambient air conditions utilizing the two-microphone technique [14, 15]. A speaker located upstream of the element being investigated generates white noise. The attenuation element is connected to the loudspeaker by a duct of internal diameter of $D = 4.859$ cm. Another tube of the same diameter is connected to the downstream end of the element and is anechoically terminated with sound absorbing material. Four 1/4-inch condenser microphones (B&K 4135) are mounted in pairs upstream and downstream of the element, flush with the tube surface to measure noise entering and exiting the element [16]. While the conditions inside the configuration tested on the impedance tube facility are quite different from the actual exhaust, the experiments yield meaningful results and trends, particularly, in terms of comparisons between the systems. Each exhaust runner of the PMMC was acoustically tested and compared with the production system for transmission loss performance, as illustrated in Figures 4–7. The runners were individually tested by connecting one runner at a time and blocking the remaining three runners at the headface with a non-anechoic termination. Such an experiment is intended to simulate the non-overlapping blow down pulse for each runner while the valves of the other runners are closed. The results, in general, show improvements for the PMMC over the production system, especially in the important low frequency range of interest below 1 kHz. These experiments

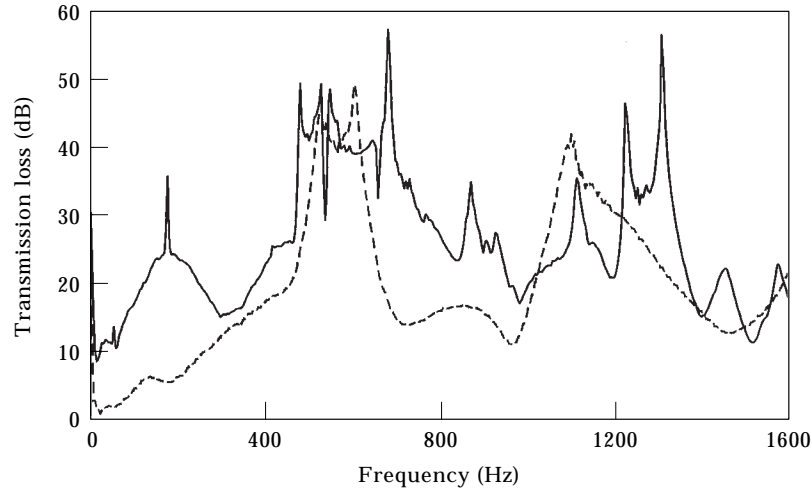


Figure 5. Transmission loss versus frequency for runner 2 of the manifold/catalyst systems: —, PMMC; ---, production.

also confirmed design estimates for the required porosity and dimensions to achieve the desired attenuation. The enhanced sound silencing performance of the PMMC is then expected to lead to a less flow restrictive muffler to be used as compared with the production system, while maintaining tailpipe noise at an acceptable level.

5. FLOWBENCH EXPERIMENTS

The flow characteristics of the PMMC exhaust system are also determined relative to the production hardware and prior to the final fabrication of the prototype for dynamometer testing. Steady flow experiments for the various

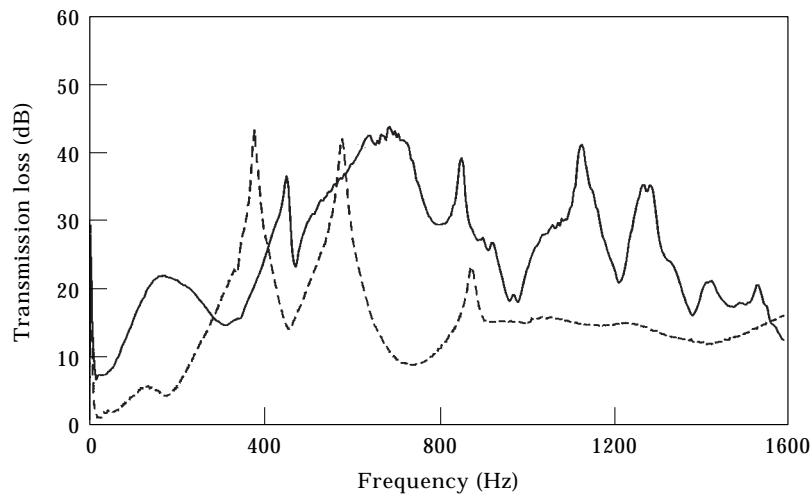


Figure 6. Transmission loss versus frequency for runner 3 of the manifold/catalyst systems: —, PMMC; ---, production.

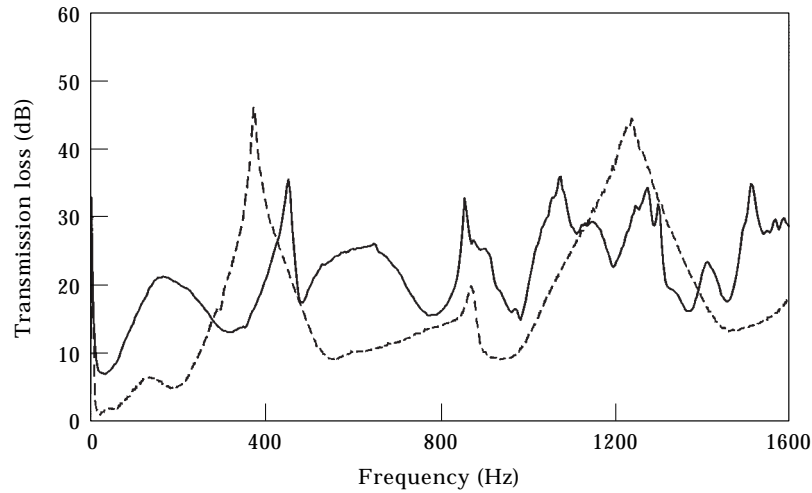


Figure 7. Transmission loss versus frequency for runner 4 of the manifold/catalyst systems: —, PMMC; ---, production.

exhaust elements were conducted with a Superflow model SF-600 flowbench, capable of producing flows of up to 600 cfm at 20" H₂O pressure drop. The major elements comprising the exhaust systems (manifold, catalyst, mufflers, resonator) were tested for steady state flow performance. Since the lengths of the two exhaust systems (production and PMMC) are retained, the viscous losses due to uniform friction will be nearly the same and may be ignored in making comparisons between the two systems. Flow loss coefficients were calculated for each component using the pressure drop across the element, normalized by the mean flow dynamic pressure $\frac{1}{2}\rho U^2$; ρ being the density and U the velocity.

The flow performance through the manifold and catalyst section of the exhaust system is determined by flowing each runner individually one at a time for each

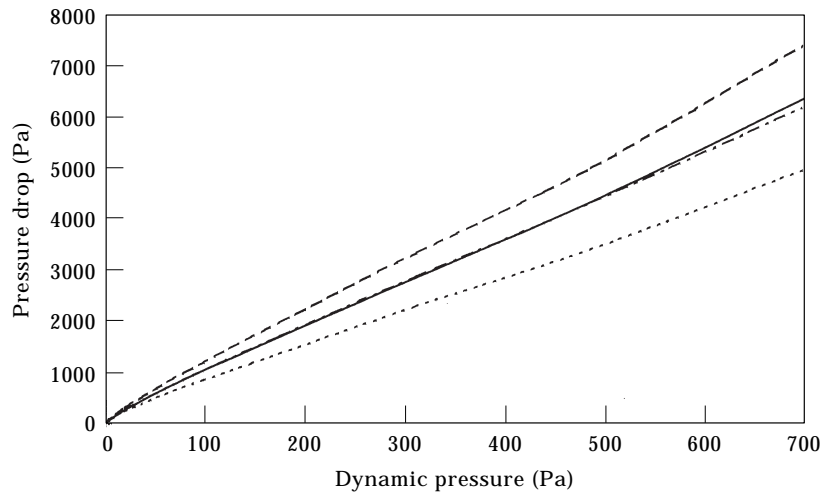


Figure 8. Pressure drop versus dynamic pressure for the production runners and catalyst: —, runner 1; ---, runner 2; ·····, runner 3; -·-·-, runner 4.

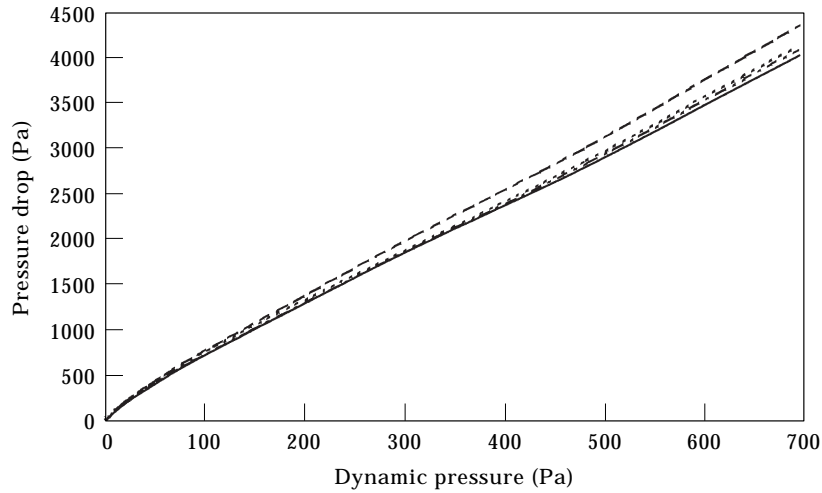


Figure 9. Pressure drop versus dynamic pressure for the PMMC runners and catalyst: —, runner 1; ---, runner 2; ·····, runner 3; -·-·-, runner 4.

system. The results are shown in Figures 8 and 9 for the production and PMMC systems, respectively. With the exception of runner No. 3, the PMMC is clearly superior to the production system. A comparison of Figures 8 and 9 also reveals that the runner losses in the PMMC system exhibit much less variability as compared with the production system. This additional uniformity will assist in reducing cylinder to cylinder differences and aid in the engine calibration process. For comparison purposes, a representative steady flow loss may also be calculated for the overall manifold/catalyst segment for both exhaust systems by averaging the pressure drops from each runner as shown in Figure 10. A comparison of the average flow loss coefficient versus flow Reynolds number is shown for each exhaust in Figure 11. Both Figures 10 and 11 show considerable improvement for

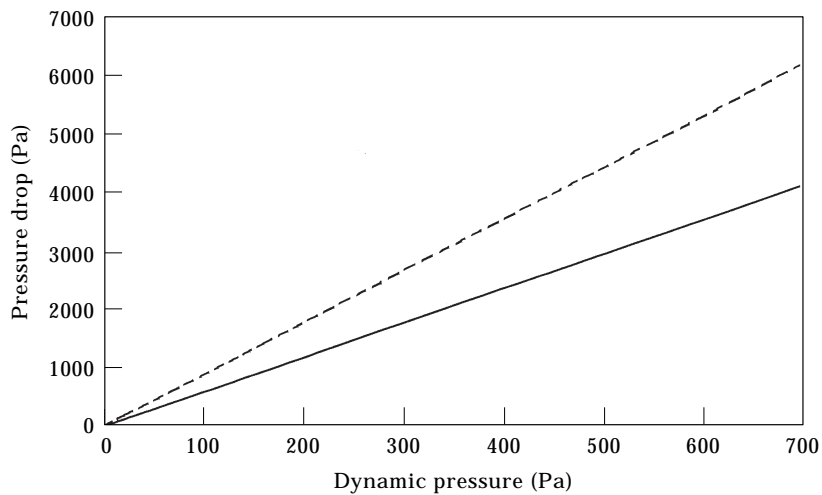


Figure 10. Runner averaged pressure drop versus dynamic pressure for comparison of the manifold/catalyst: —, PMMC; ---, production..

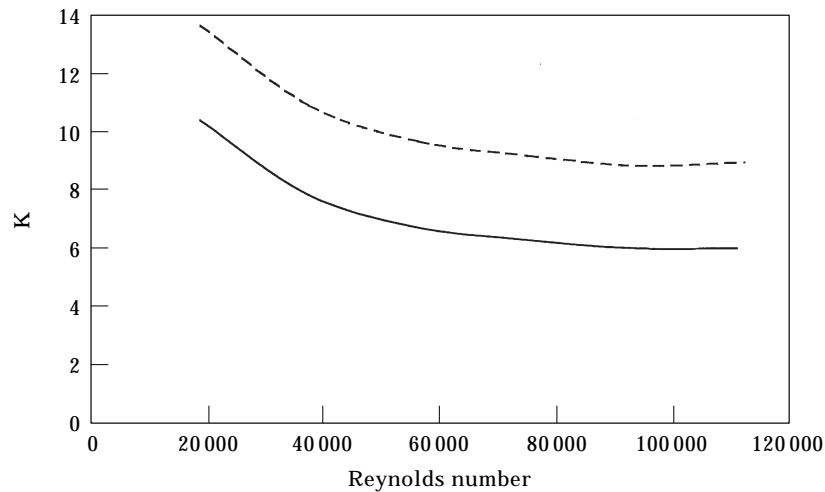


Figure 11. Runner averaged flow loss coefficient versus Reynolds number for comparison of the manifold/catalyst: —, PMMC; ---, production.

the PMMC system. While this approach ignores runner interactions, in reality there is little flow overlap between runners. Therefore, an average of the steady flow loss coefficient from each runner of the manifold/catalyst is expected to give a reasonable comparison between systems. Flow losses through the mufflers of each exhaust system were measured as well, as shown in Table 1. The data reveals the potential benefits of replacing the production muffler with the low restriction muffler.

Adding the component flow loss coefficients, and ignoring the pipe lengths connecting the components, the total loss coefficient for each exhaust system may be determined, as also shown in Table 1. To summarize, neglecting frictional losses in the pipes and moving downstream from the headface to the tailpipe exit, loss coefficients for the production system total 19.8 while that of the PMMC system total 11.1, a 44% reduction. Thus, the PMMC system has superior steady state performance as compared with the production system, which supports the preliminary estimates made early in the design process of the prototype PMMC system. Having performed favorably in terms of flow efficiency and acoustic

TABLE 1

Summary of measured total flow loss coefficients

	Production	PMMC
Manifold/catalyst	9.2	6.3
Resonator	1.3	—
Muffler	9.3	4.8
Total	19.8	11.1

attenuation, the PMMC system was finalized and fabricated for fired engine experiments.

6. ENGINE DYNAMOMETER EXPERIMENTS

The PMMC concept is compared with the production exhaust system of the 1992 Ford 1.9L I4 (Escort) engine. All other engine parameters are maintained to ensure that the differences in exhaust noise levels, engine performance, and pollutant emissions may be attributed strictly to the variations in the exhaust system design. A surge tank is utilized at the tailpipe exit to maintain steady pressure conditions at the outlet.

Engine Dynamometer experiments were conducted to assess operational performance during Wide Open Throttle (WOT), cold start warm-up, and simulated driving schedules. The tests have been named: Wide Open Throttle rpm map (WOT map), Cold Start, and Federal Test Procedure (FTP). Each of the test procedures provides unique and necessary data to properly evaluate the performance of the proposed PMMC design.

The experiments used a General Electric regenerative electric dynamometer controlled by a Dyne Systems digital controller. Throttle position is controlled via the Dyne Systems digital throttle controller. Commands to the controllers are initiated by Horiba Instruments Data Acquisition and Engine Control System Software installed on a Unix computer. The software program is a complete engine controller and signal acquisition system capable of acquiring data up to 10 Hz, while fully controlling engine operation. Signals from such devices as thermocouples, differential pressure transducers, fuel metering, analyzers, and slow time response pressure transducers are processed and calibrated using this software. The emission bench is capable of analyzing engine-out oxygen (O_2), carbon monoxide (CO), carbon dioxide (CO_2), hydrocarbons (HCs), and nitrogen oxide (NO_x) concentrations in the exhaust flow.

A Concurrent 7250 high speed data acquisition system, shown in Figure 12, allows the simultaneous recording of pressure data as a function of time from up to 32 locations on the engine exhaust systems. Kistler piezoresistive pressure transducers connected to digital amplifiers were used to measure the absolute pressures. The computer system acquires and time stamps the amplified signals with the aid of timing signals. A signal to mark the start and completion of an engine cycle (based on Top Dead Center (TDC) of cylinder No. 1) is provided by a proximity sensor mounted adjacent to the camshaft pulley producing a pulse per engine cycle. Sampling is acquired at each crank angle degree using a signal supplied by an optical encoder connected to the crankshaft at the front of the engine. An optical isolator is used to filter out noise in both timing signals. Data is averaged over 64 engine cycles to avoid cyclic variations. The pressure versus time data is then post-processed to obtain relevant pressure versus time plots as well as mean pressure levels for flow loss assessment.

Attenuation performance was measured during steady state engine operation at WOT and various rpm set points. The pressure versus time data was acquired at several locations within the exhaust system. Locations of particular interest

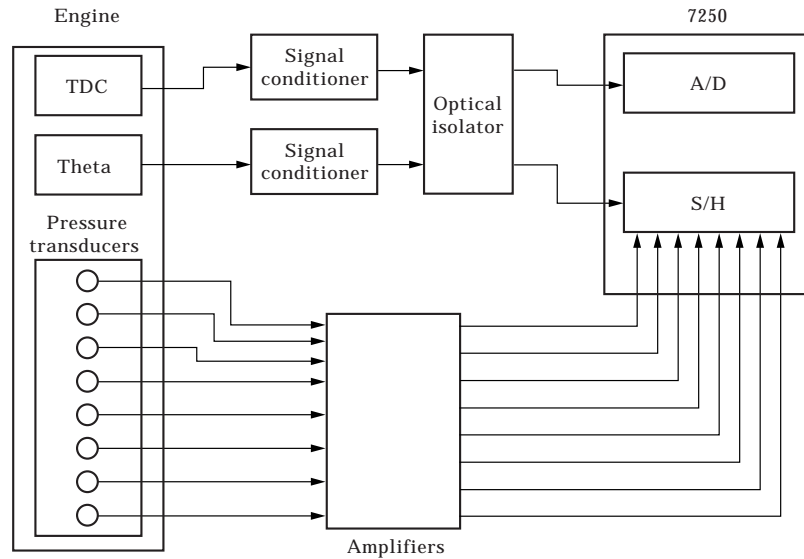


Figure 12. Schematic of the high speed pressure data acquisition system.

were: (1) exhaust port No. 1 at the headface, (4) just after the catalyst, and (8) at the tailpipe exit, as shown in Figure 2. The data is then Fourier transformed to the frequency domain to determine sound pressure levels (SPL) at various locations. Mean averaged values of the pressure data are also used for an approximate assessment of pressure drop across the elements and along the system.

Exhaust gas pressure variations as a function of crank angle are compared for each of the exhaust systems in Figures 13–15 at 1000, 3000, and 5000 rpm for locations 1, 4, and 8. Four distinct peaks are observed in each figure due to the 4 blowdown pulses per cycle. For 1000 rpm, Figure 13 (a–c) shows that the pressure amplitudes at location 1, corresponding to the headface, are reduced significantly for the PMMC system as compared with the production system. The overall pressure wave amplitude decreases in the downstream direction for both systems, while the improvement of PMMC system is observed to persist after the catalyst (location 4) and even after the muffler (location 8). As engine speed is increased to 3000 rpm and then 5000 rpm, pressure wave amplitudes are observed to increase but similar trends for the advantages of the PMMC remain. As engine speed is increased, the PMMC system provides even more substantial reductions in the magnitude of pressure fluctuations over the production system. These reductions in the exhaust system translate directly to lower SPLs with the PMMC system. Figure 16(a–c) compares the overall SPL in the duct by location at 1000, 3000, and 5000 rpm, respectively. The figures show the increase of engine source SPL with the rpm and the decrease in SPL in the flow direction as a result of exhaust system attenuation. Location 8, which is essentially the tailpipe exit, shows lower SPL for the PMMC system as compared with that of the production system.

A frequency domain analysis of the sound pressure data by location and rpm indicates that the predominant SPLs can be attributed to low frequency

components of blowdown and its harmonics. As expected, the predominant orders correspond to the blowdown frequency of 2 events per revolution (second order). Because sound levels are plotted in decibel units, only the first several peaks of sound pressure level are significant in assessing the total sound pressure level. Therefore, sound levels are commonly plotted versus the first several engine orders. The comparisons of the SPL data versus order at locations 1, 4 and 8 for 1000,

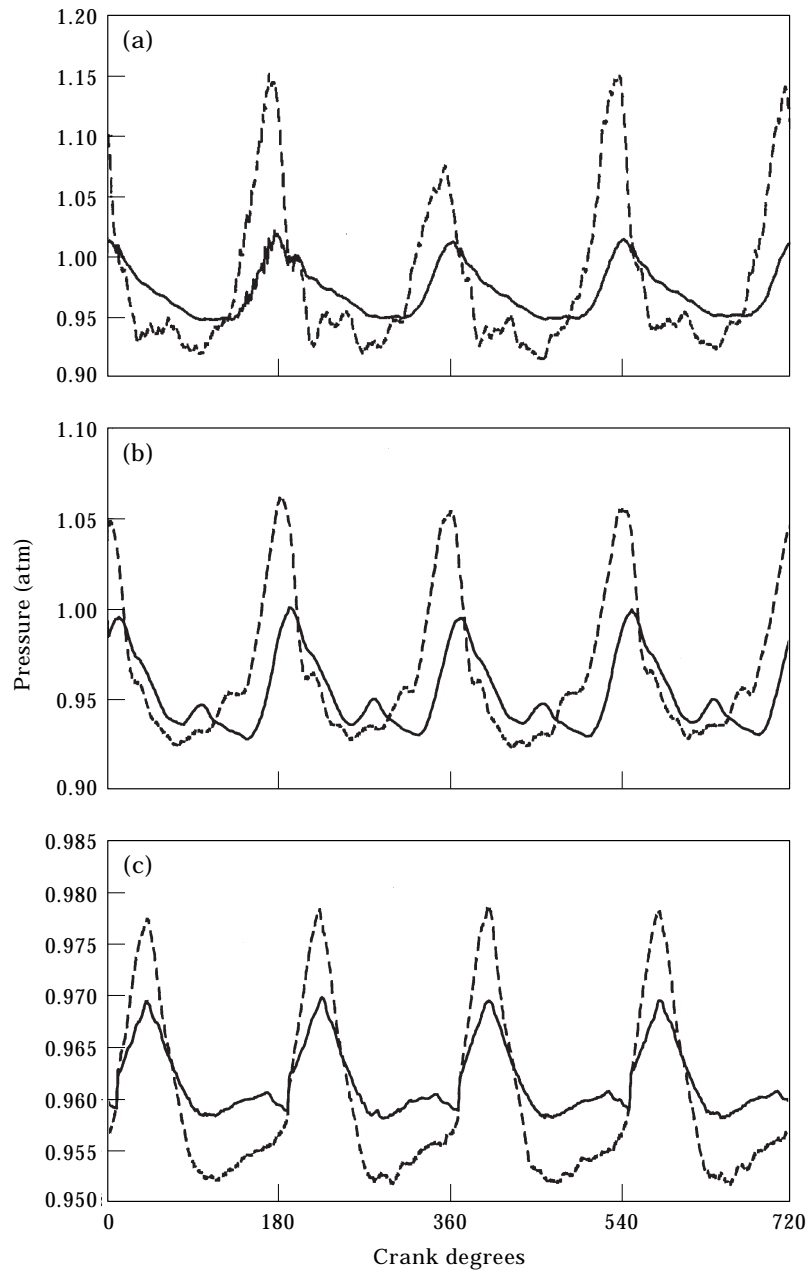


Figure 13. Pressure versus crank angle at 1000 rpm and locations: (a) 1, (b) 4, and (c) 8 to compare exhaust system effects: —, PMMC; ---, production.

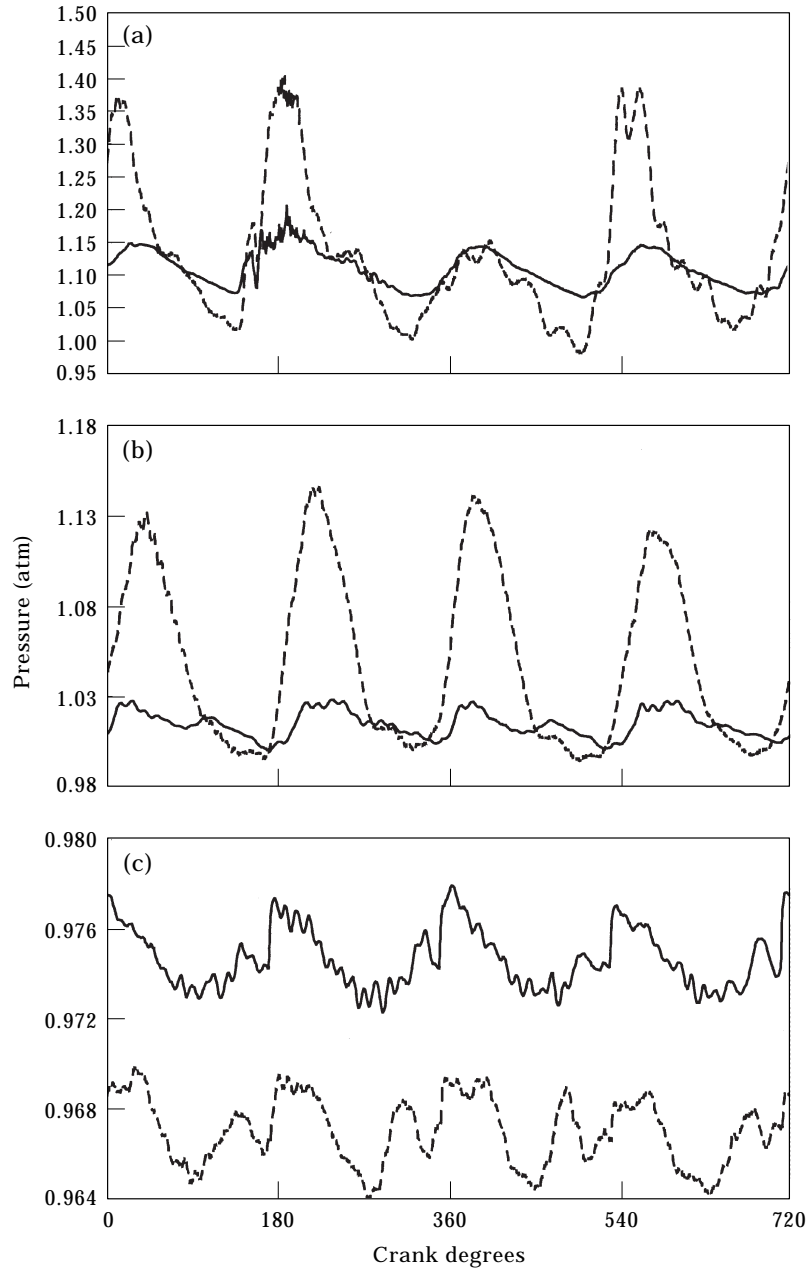


Figure 14. Pressure versus crank angle at 3000 rpm and locations: (a) 1, (b) 4, and (c) 8 to compare exhaust system effects: —, PMMC; ---, production.

3000, and 5000 rpm are shown in Figures 17–19. The upstream manifold volume of the PMMC system reduces sound pressure levels as compared with the production system at locations 1 and 4, while maintaining the level at location 8. The data shows an increase in sound pressure level with rpm due to increased pressure amplitudes, as depicted for location 1 in Figure 17(a), 18(a), and 19(a) at 1000, 3000, and 5000 rpm, respectively. The expected decrease in SPL in the flow

direction due to exhaust system attenuation can be readily observed at 5000 rpm in Figure 19(a-c) at locations 1, 4, and 8, respectively. The PMMC provides improvement in noise reduction over the production system at all locations. This improvement is most significant at high rpms during the generation of high levels of exhaust noise.

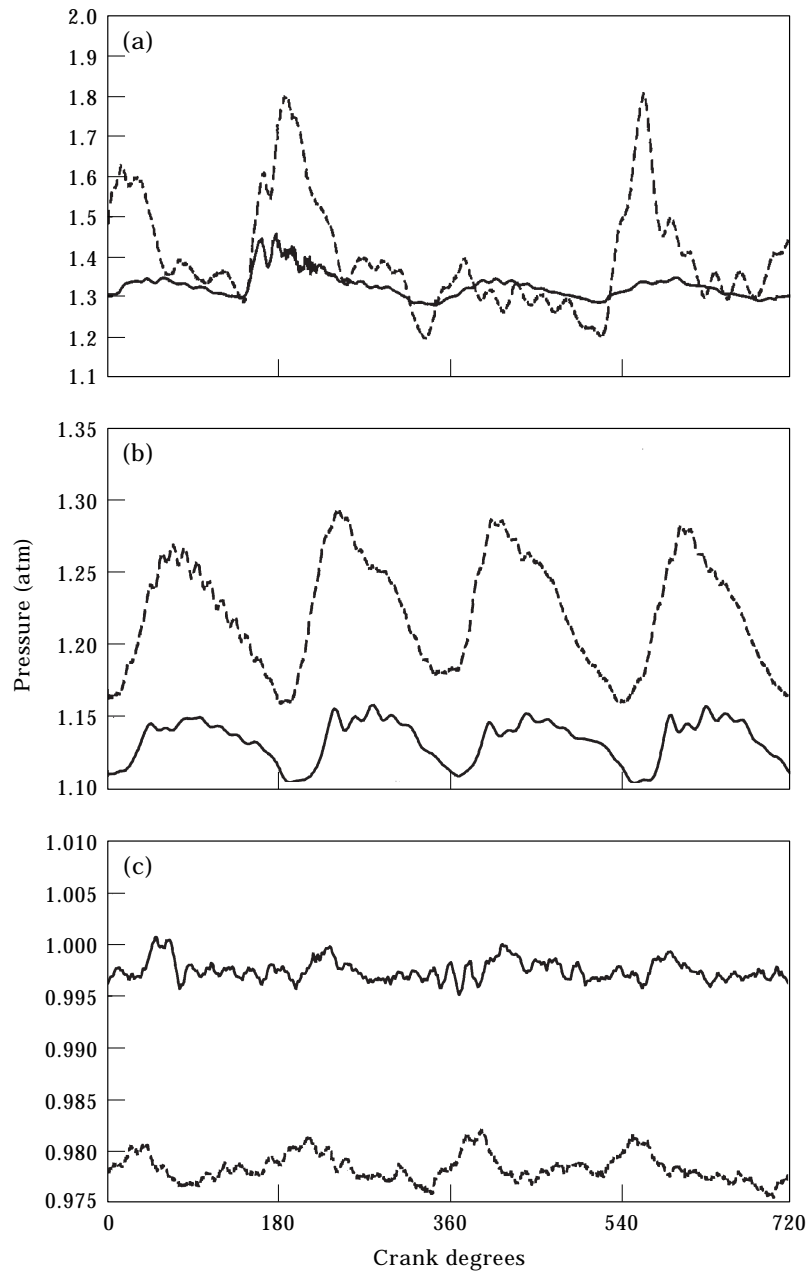


Figure 15. Pressure versus crank angle at 5000 rpm and locations: (a) 1, (b) 4, and (c) 8 to compare exhaust system effects: —, PMMC; ---, production.

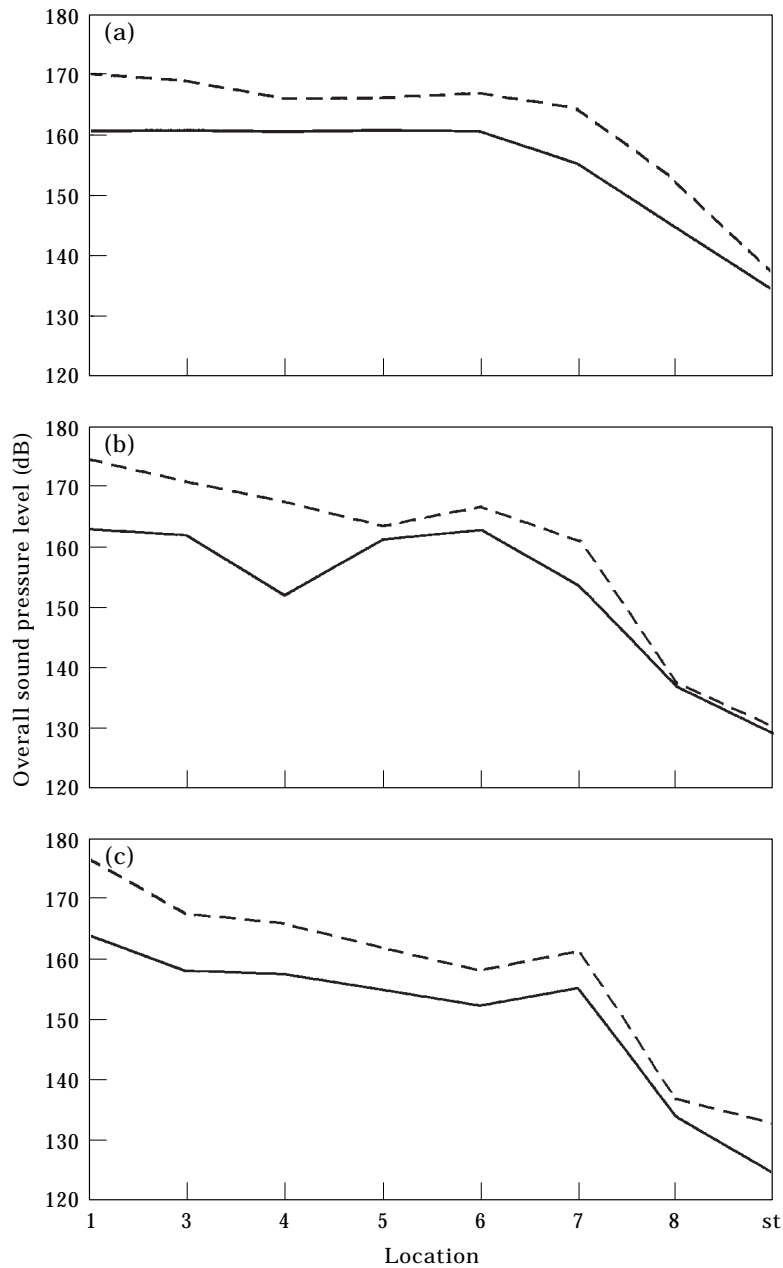


Figure 16. Overall sound pressure level versus location at (a) 1000, (b) 3000, and (c) 5000 rpm to compare exhaust system effects: —, PMMC; ---, production.

The foregoing experimental evaluations of the acoustic properties agreed with computational simulations conducted with Ford's Manifold Dynamics engine simulation code—MANDY [17]. This code provided additional confirmation of the attenuation and enhanced engine performance due to the PMMC system. Because of space concerns, the details of the computational simulations have been excluded from this work [1].

Steady state WOT maps were used to assess the engine output because they are the standard by which automotive manufacturers typically gauge engine performance in terms of such measurables as torque, horsepower, and volumetric efficiency. By maintaining the rest of the engine system constant while varying only the exhaust system, accurate evaluations can be made of the exhaust system effects on engine performance. Absolute, time-dependent pressure measurements are

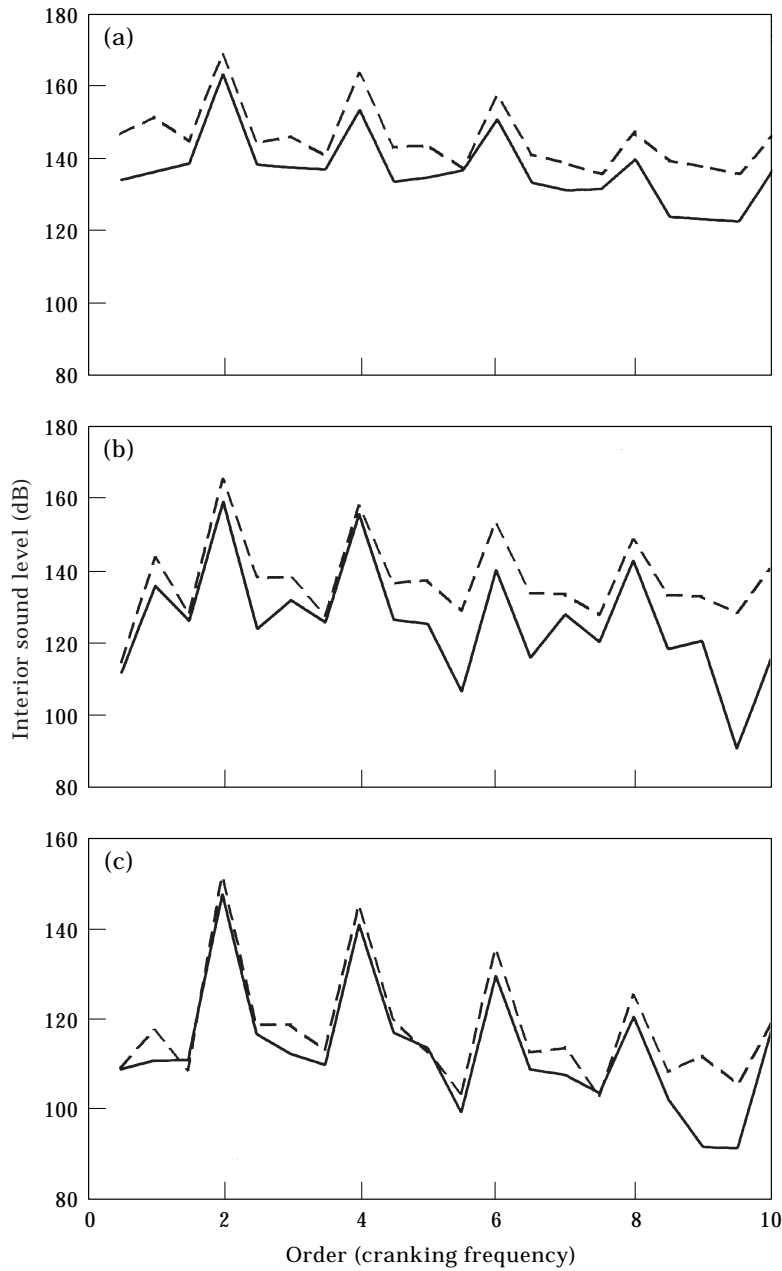


Figure 17. Sound pressure level versus order at 1000 rpm and locations: (a) 1, (b) 4, and (c) 8 to compare exhaust system effects: —, PMMC; ---, production.

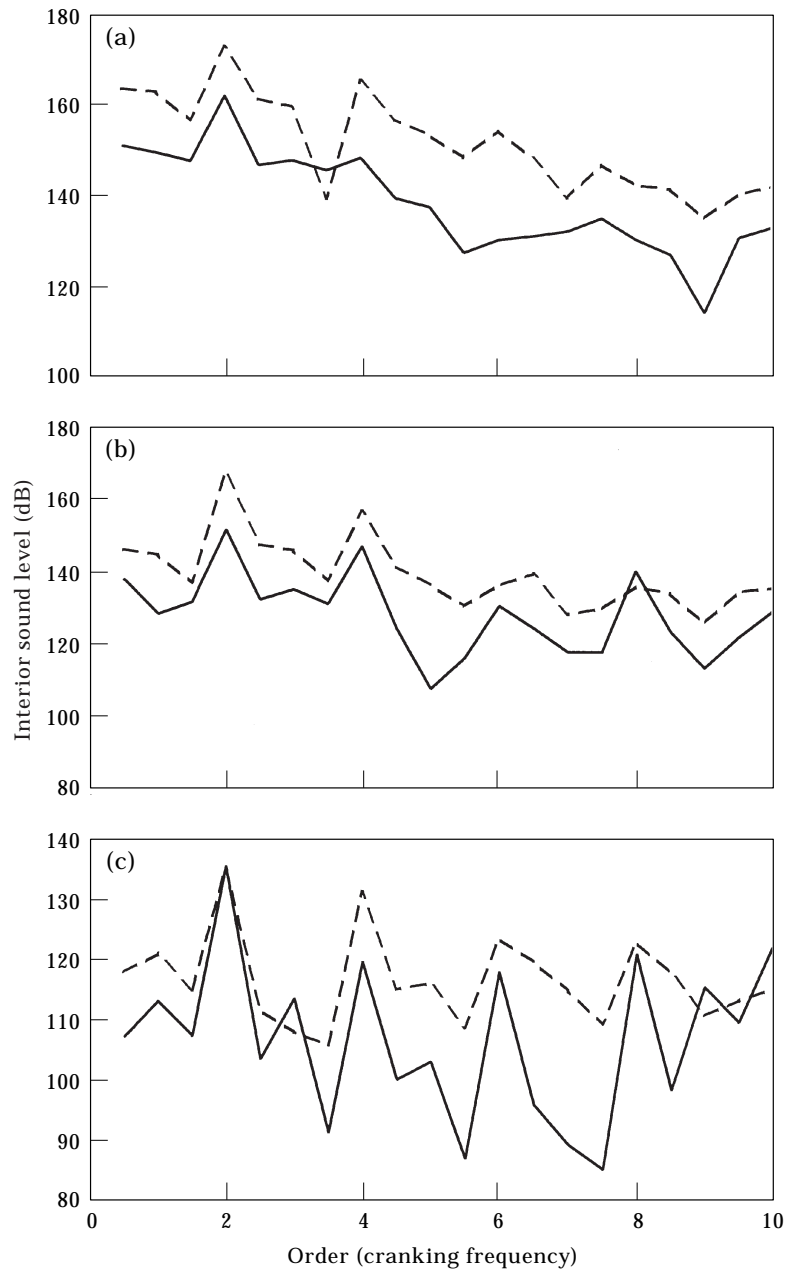


Figure 18. Sound pressure level versus order at 3000 rpm and locations: (a) 1, (b) 4, and (c) 8 to compare exhaust system effects: —, PMMC; ---, production.

averaged by location to determine mean pressure levels within each exhaust system. The mean pressure information helps identify the sources of head losses within the exhaust system.

Table 2 summarizes the brake torque averaged over numerous experiments for the exhaust systems and shows gains in engine performance due to the PMMC exhaust system. This is a result of reduced back pressure as elaborated next.

Pressure drop increases with flow rate, therefore the increased back pressure is most appreciable at high rpms. For example, Figure 20 shows mean pressure levels for 5000 rpm at various exhaust locations from the headface to the exit at the surge tank. The differences in mean pressure at location 1 between systems and the large flow losses associated with the mufflers (location 7–8) are more pronounced at 5000 rpm due to increased flow separation. The mean pressure level

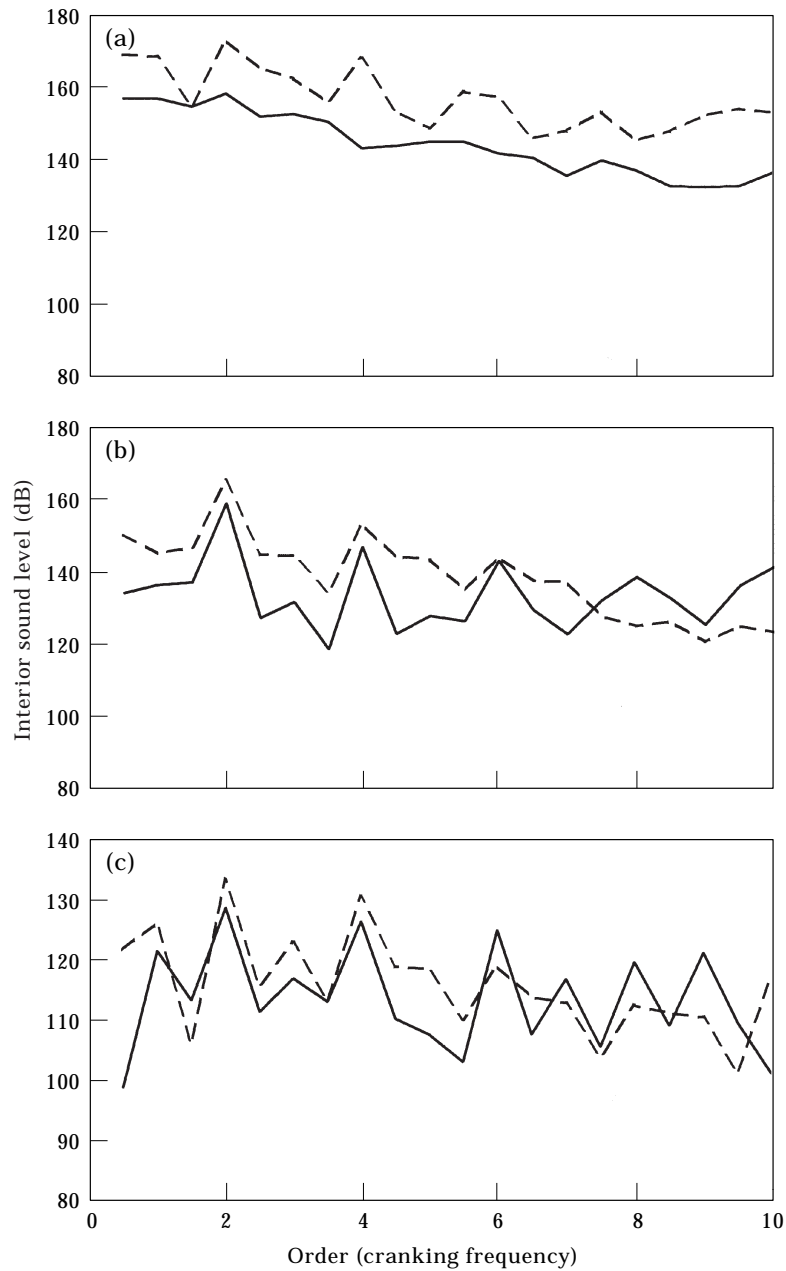


Figure 19. Sound pressure level versus order at 5000 rpm and locations: (a) 1, (b) 4, and (c) 8 to compare exhaust system effects: —, PMMC; ---, production.

TABLE 2
Summary of measured brake torque (units are in N-m)

rpm	Production	PMMC
1000	100.3	102.8
1500	110.6	112.5
2000	118.9	120.1
2500	124.9	127.6
3000	121.3	123.2
3500	124.6	127.6
4000	122.7	126.0
4500	112.0	117.5
5000	102.1	106.2
5500	83.7	87.3

at the headface of exhaust runner 1 is higher for the production system than in PMMC. This creates increased engine back pressure and thereby reduces the available brake torque of the production system.

Emission results were based on cold start warm-up tests and FTP drive simulations [18, 19]. Cold start testing showed faster catalyst warm-up for the PMMC system by nearly 40%. Because nearly half of the total pollutants are produced during the first 6 min of the 22 min simulated drive schedule, improved light-off time also reduced total emissions for the drive. Reduction of 16, 27 and 9% were found for carbon monoxide, hydrocarbons, and nitrogen oxides, respectively.

Fired engine experiments showed improvements for the PMMC system in virtually all evaluation areas, including: noise levels, brake torque, catalyst light-off, and total pollutant emissions. The total vehicle weight would also be

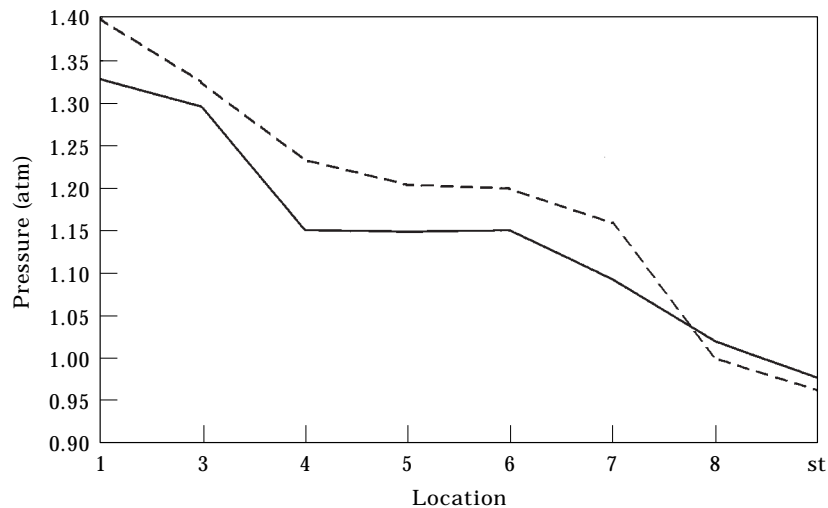


Figure 20. Mean pressure versus location at 5000 rpm to compare exhaust system effects: —, PMMC; ---, production.

TABLE 3
Exhaust component mass summary
 (units are in kg)

	Production	PMMC
Manifold/catalyst	11.2	11.6
Resonator	2.2	–
Muffler	4.3	3.4
Total	17.7	15.0

reduced as a result of total exhaust system weight reductions, as shown in Table 3. Note that due to somewhat crude fabrication methods, the PMMC prototype is heavier than would be possible utilizing conventional production methods. This reduction would have a small, but positive impact on the fuel economy.

7. CONCLUSIONS

A new exhaust manifold design, the PMMC concept, is studied, which provides upstream sound silencing through the use of a perforated exhaust manifold and expansion chamber system. The estimated acoustic improvements were examined by experimental studies, which showed substantial noise reduction in the manifold volume, enabling the use of a less restrictive muffler, while maintaining the original sound output levels. The acoustic improvements are combined with the enhancements in engine performance due to reduced back pressure. Results showed an approximate 30% reduction of exhaust back pressure, which improved wide open throttle torque by 3 to 5% as a result of the reduced pumping work. The increased torque provides improved vehicle acceleration response and can enhance fuel efficiency if properly utilized in the design of the powertrain system. The concept also reduces the catalyst light-off time by nearly 25%, yielding improvements in cold start emissions. Experimental studies demonstrated that the PMMC design reduces total pollutant emissions by more than 15% as a result of improved cold start emissions.

The PMMC concept also reduces total exhaust system weight by approximately 15%. The resonator has been eliminated; the muffler has been simplified; and the manifold and catalyst have been combined into a single part, possibly reducing the exhaust system complexity. The improvements in engine output power and the corresponding fuel efficiency improvement may translate to considerable savings. Thus, the PMMC design, in general, is expected to have additional merits over the conventional approaches.

REFERENCES

1. K. R. NORMAN 1996 *Ph.D. Thesis, The University of Michigan*. Investigation and design of an alternative exhaust system for minimum noise, pollutant emissions, and power loss, a theoretical, computational, and experimental approach.

2. A. SELAMET, N. S. DICKEY and J. M. NOVAK 1995 *Journal of Vibration and Acoustics* **117**, 323–331. A time-domain computational simulation of acoustic silencers.
3. D. E. BAXA 1969 *Noise Control in Internal Combustion Engines*. Malabar, FL: Robert E. Krieger Publishing.
4. C. F. TAYLOR 1990 *The Internal Combustion Engine in Theory and Practice*, Volume 1. Boston, MA: The M.I.T. Press.
5. D. D. DAVIS, G. M. STOKES, D. MOORE and G. L. STEVENS 1954 *NACA TN* 1192. Theoretical and experimental investigations of mufflers with comments on engine exhaust muffler design.
6. N. S. DICKEY, A. SELAMET and J. M. NOVAK 1996 *SAE* 960307. A time domain-based computational approach for perforated tube silencers.
7. A. SELAMET, N. S. DICKEY and J. M. NOVAK 1997 *Journal of the Acoustical Society of America* **101**, 41–51. Circular concentric Helmholtz resonators.
8. C. I. J. YOUNG 1973 *Ph.D. Thesis, Purdue University*. Acoustic analysis of mufflers for engine exhaust systems.
9. J. W. SULLIVAN and M. J. CROCKER 1978. *Journal of the Acoustical Society of America* **64**, 207–215. Analysis of concentric-tube resonators having unpartitioned cavities.
10. A. SELAMET and P. M. RADAVIDH 1997 *Journal of Sound and Vibration* **210**, 407–426. The effect of length on the acoustic attenuation performance of concentric expansion chambers: an analytical, computational, and experimental investigation.
11. M. ALSTER 1972 *Journal of Sound and Vibration* **24**, 63–85. Improved calculation of resonant frequencies of Helmholtz resonators.
12. Y. FUKAE 1991 *SAE* 910303. The development of lightweight and low-heat-capacity exhaust manifolds.
13. A. J. BAXENDALE 1993 *SAE* 931072. The role of computational fluid dynamics in exhaust system design and development.
14. J. Y. CHUNG and D. A. BLASER 1980 *Journal of the Acoustical Society of America* **64**, 907–913, 914–921. Transfer function method of measuring in-duct acoustic properties: I, theory, II, experiment.
15. ASTM E 1050-90 1990 *American Society for Testing and Materials, Philadelphia, PA*. Standard test method for impedance and absorption of acoustical materials using a tube, two microphones, and digital frequency analysis system.
16. A. SELAMET, N. S. DICKEY and J. M. NOVAK 1993 *Presented at NOISE-CON 93, Fort Lauderdale, FL*. A time domain based computational approach for perforated tube silencers.
17. M. CHAPMAN, J. M. NOVAK and R. A. STEIN 1982 in *Flows in Internal Combustion Engines, ASME WAM* (T. Uzkan, editor). Numerical modeling of inlet and exhaust flows in multi-cylinder internal combustion engines.
18. N. K. HYATT 1996 *Masters Thesis, The University of Michigan*. A turbulent flame entrainment and burning model for in-cylinder combustion: implementation into an engine simulation code.
19. *U.S. Code of Federal Regulations* 1995 **40**, part 86. EPA Urban Dynamometer Driving Schedule.